Development of Test-Analysis Models for Large Space Structures Using Substructure Representations

Daniel C. Kammer*
University of Wisconsin, Madison, Wisconsin 53706
and
Christopher C. Flanigan†
SDRC, Inc., San Diego, California 92121

A method is presented for reducing a substructured finite element model to a test-analysis-model representation for use in test-analysis correlation. The method requires sensor locations within each substructure to be selected such that they are capable of spatially differentiating between the component mode shapes of the substructures rather than an analogous requirement of an earlier method pertaining to the system mode shapes. This is an important development for FEM representations of large space structures that are often formed of extremely detailed substructures with weak coupling. The new method was applied to a simple but representative example of a model containing three substructures. A straightforward application of the earlier method of model reduction resulted in the inability to spatially differentiate between the system mode shapes at the substructure level. The new reduction method for substructured models resulted in a test-analysis model that exactly predicted the finite element model frequencies and mode shapes to within numerical accuracy.

Introduction

TODAY'S complex spacecraft require accurate analytical models for use in both structural dynamic analysis and control law synthesis. When considering proposed large space structures (LSS), the required finite element models (FEM) can possess hundreds of thousands of degrees of freedom. To reduce the size of these models, a structural dynamicist will usually pick a frequency range of interest, transform the system to modal space, and eliminate all structural modes with frequencies outside the specified range. A control dynamicist will, in general, reduce the model further by examining an appropriate state-space and eliminating states that are determined to be unimportant based upon some performance criteria. However, there are cases of interest where the FEM must be reduced in physical space to a relatively small number of degrees of freedom that will be used to describe system response. This type of reduced model is required in the area of test-analysis correlation and system identification.

Before one can use an FEM to obtain accurate predictions of LSS loads and response, it must be validated using experimental data obtained from a vibration test of the structure. In many cases, ground vibration tests can be performed, even for relatively large structures, such as the Space Shuttle solid rocket booster.[1,2] However, in the case of LSS such as the proposed space station, on-orbit system identification will have to be performed due to structural size and flexibility. In either case, the accuracy of the corresponding FEM can be determined by comparing responses predicted by the model with responses measured during a vibration test. Rather than comparing responses directly, an FEM is usually validated by comparing analytical modal parameters, such as frequency and mode shapes, with modal parameters obtained from the test response data.

Received Oct. 20, 1989; revision received Sept. 15, 1990; accepted for publication Sept. 17, 1990.

*Assistant Professor, Department of Engineering Mechanics. Senior Member AIAA.

†Director of Aerospace Projects. Member AIAA.

Test and FEM modal frequencies can be compared directly. Corresponding mode shapes are compared in an indirect manner using shape correlation measures, such as orthogonality, cross-orthogonality, modal effective mass distributions, and modal kinetic energy distributions, as described in Ref. 3. Each of these correlation techniques uses an analytical mass matrix for weighting. The dynamically important degrees of freedom are, therefore, emphasized in the correlation based upon mass distribution. If the two sets of modal data correlate to the desired level of accuracy for all of the dynamically important modes, the FEM can be considered validated. However, if the analytical mode shapes and frequencies do not agree with the test data, methods must be used to correct the FEM, such as those presented in Refs. 2–6.

Although the FEM and test frequencies can be directly compared, corresponding mode shapes cannot be directly used in the shape correlation measures due to the mismatch between the number of degrees of freedom in the FEM and the number of sensors placed on the structure during testing. There are two approaches that one can take to remedy this situation. The first approach expands the test mode shapes from test-size to FEM-size using the FEM mass and stiffness matrices.[5] This procedure has a severe drawback in that errors present in the FEM that we are trying to identify are introduced into the test modes that we are assuming reflect reality. This corruption of the test data will, in general, lead to errors in the model validation process. In addition, the expansion process can be computationally intensive because a matrix decomposition is required for each test mode expanded.

The second approach uses a transformation matrix to reduce the FEM to the degrees of freedom that are monitored during the test. The reduced representation is called a test-analysis model (TAM). There will be a one-to-one relationship between test degrees of freedom and TAM degrees of freedom; therefore, the TAM mode shapes and mass matrix can be used directly with the test modes in the shape correlation measures.

If the test-TAM frequency and mode shape correlation are to yield useful information concerning the accuracy of the FEM, the TAM must accurately represent the dynamic characteristics of the FEM in the frequency range of interest. In the past, reduction to the TAM level was typically accomplished using Guyan or static reduction.[3,8-10] Recently a new method called modal reduction was introduced in Ref. 11. This reduc-

tion method uses the already computed FEM mode shapes to reduce the FEM mass and stiffness matrices to the degrees of freedom at the sensor locations. The method offers a distinct advantage in that the TAM will exactly (within the accuracy of the computer) predict the FEM mode shapes and frequencies. All reduction error is eliminated from the test-analysis correlation procedure. The method has been successfully used on several space structures, where the static reduction failed to give accurate results.[2,11]

Modal reduction was originally developed for a FEM that is small enough to be analyzed without using substructuring techniques. However, due to the size of LSS FEM representations, models must be split into many substructures. The method presented in Ref. 11 can be extended for application to a substructured FEM. The extended method has been successfully applied to a substructured model in the FEM validation for the Space Shuttle solid rocket booster.[1] However, in some cases, the extended method has failed for substructured models resulting in a very inaccurate TAM. The purpose of this paper is to briefly review the application of modal reduction to FEM representations that are not substructured, extend the formulation to substructured models, and identify the errors that can result from this application. A new reduction formulation is then presented for substructured models that eliminates the problem. A realistic application of the new method is also presented.

Reduction of a Nonsubstructured FEM

The equation of motion for an undamped n degree-of-freedom FEM representation is given by

$$M_n \ddot{u}_n + K_n u_n = F_n \tag{1}$$

where M_n and K_n are the system mass and stiffness matrices, u_n is the physical displacement vector, and F_n is a vector containing the applied loads. The corresponding eigenvalue equation is of the form

$$-M_n \Phi_n \omega_n^2 + K_n \Phi_n = 0 \tag{2}$$

in which Φ_n is a modal matrix and ω_n^2 is a diagonal matrix containing the corresponding system frequencies.

The objective of the TAM generation process is to reduce the system described by Eq. (2) to a representation containing r degrees of freedom while maintaining the dynamic integrity of the original system in the frequency range of interest. The r degrees of freedom will be monitored during the modal survey and, in general, $r \ll n$ due to the limited availability of sensors. If we consider only the ith mode shape and partition all matrices and vectors into complementary sets a and o, we get a matrix equation of the form

$$-\omega_i^2 \begin{bmatrix} M_{aa} & M_{ao} \\ M_{oa} & M_{oo} \end{bmatrix} \begin{bmatrix} \Phi_{ia} \\ \Phi_{io} \end{bmatrix} + \begin{bmatrix} K_{aa} & K_{ao} \\ K_{oa} & K_{oo} \end{bmatrix} \begin{bmatrix} \Phi_{ia} \\ \Phi_{io} \end{bmatrix} = 0 \tag{3}$$

Degrees of freedom in the a set will be retained in the TAM representation; the o-set degrees of freedom will be eliminated using a transformation.

Solution of the lower partition of Eq. (3) results in a transformation matrix $T_i = [I : D_i^T]^T$ that relates the ith FEM mode shape to its a-set partition

$$\Phi_i = T_i \Phi_{ia} \tag{4}$$

where

$$D_i = [-\omega_i^2 M_{oo} + K_{oo}]^{-1} [\omega_i^2 M_{oa} - K_{oa}] \tag{5}$$

Transformation T_i can be used to reduce the FEM mass and stiffness matrices to the TAM level via the relations

$$M_{ir} = T_i^T M_n T_i \qquad K_{ir} = T_i^T K_n T_i \tag{6}$$

TAM mass and stiffness matrices M_{ir} and K_{ir} satisfy the eigenvalue equation for the a-set partition of the ith FEM mode shape

$$[-M_{ir} \omega_i^2 + K_{ir}] \Phi_{ia} = 0 \tag{7}$$

The desired product of the reduction procedure is the TAM mass matrix M_{ir}, which is used as a weighting matrix in test-analysis mode shape correlation. The transformation represented by Eq. (5) has been used extensively in dynamic condensation applied to component mode synthesis.[12–14] It is less successful at producing a usable TAM mass matrix. The reduction is valid only at the single frequency ω_i, and the reduced mass and stiffness matrices will only accurately characterize the ith FEM mode shape. Experience has shown that accuracy falls off dramatically on either side of the reduction frequency. A TAM generated using the transformation of Eq. (5) would have to be produced for each FEM modal frequency. Clearly, this type of reduction is inadequate for test-analysis correlation purposes.

A useful reduction transformation must relate the omitted degrees of freedom to the retained degrees of freedom in a manner independent of frequency, such that one TAM can be used for the entire frequency range of interest. If we neglect the frequency dependent terms in Eq. (5), we get the familiar Guyan,[15] or static reduction, given by

$$D_s = -K_{oo}^{-1} K_{oa} \tag{8}$$

The columns of static transformation $T_s = [I : D_s^T]^T$, called constraint modes,[16] represent deflections of the omitted degrees of freedom when one of the a-set degrees of freedom is given a unit deflection while the remaining a-set degrees of freedom are constrained. If the FEM mode shapes in the frequency range of interest can be expressed as linear combination of these static shapes, the static TAM will accurately represent the FEM dynamics. In some situations, the static reduction is accurate for a relatively small number of retained degrees of freedom, or sensor locations. However, if the structure possesses large mass-to-stiffness ratios, the terms omitted in the static reduction will be nontrivial. An accurate static TAM will then require an excessive number of retained degrees of freedom. The inaccuracy of a static TAM was illustrated for a solid rocket motor in Ref. 2.

Modal reduction was introduced in Ref. 11 as an alternative to static reduction. The method is based upon the modal transformation

$$u_n = \Phi_n q \tag{9}$$

Equation (9) can also be partitioned into the complimentary a and o sets, resulting in two expressions

$$u_a = \Phi_a q \qquad u_o = \Phi_o q \tag{10}$$

for the physical displacements of the a-set and o-set degrees of freedom in terms of the generalized modal coordinates q. The objective is to determine a transformation matrix D_m that relates u_o to u_a. We can combine Eqs. (10) by eliminating the generalized coordinate vector q. Premultiplying the first of Eqs. (10) by Φ_a^T and then inverting the matrix $\Phi_a^T \Phi_a$ yields an expression for q given by

$$[\Phi_a^T \Phi_a]^{-1} \Phi_a^T u_a = q \tag{11}$$

where $[\Phi_a^T \Phi_a]^{-1} \Phi_a^T$ represents the Moore-Penrose generalized inverse[17] of Φ_a, which, in general, is a rectangular matrix possessing r rows and m columns.

Solution of q requires that the matrix Φ_a is full column rank. Therefore, there must be enough sensors on the structure to render the m columns of Φ_a linearly independent. This is a prerequisite for any accurate TAM representation. A TAM

must possess enough degrees of freedom to spatially distinguish between the modes that are to be correlated. The columns of Φ_a will always be linearly independent, and the inverse of $\Phi_a^T\Phi_a$ will always exist for a well-posed TAM. Therefore, the linear independence constraint is not a limitation of the modal reduction method when it is applied to a nonsubstructured FEM.

Equation (11) is substituted into the second of Eqs. (10), yielding the relation

$$u_o = \Phi_o[\Phi_a^T\Phi_a]^{-1}\,\Phi_a^T\,u_a = D_m\,u_a \tag{12}$$

where D_m is the desired transformation from the a set to o set. Equation (12) represents the displacement of the omitted degrees of freedom as a linear combination of the omitted partitions of the FEM mode shapes of interest.

Matrix D_m is independent of frequency, therefore, the transformation $T_m = [I:D_m{}^T]^T$ can be used to reduce the FEM mass and stiffness matrices, using expressions analogous to Eq. (6). Transformation T_m possesses all of the information contained in the FEM mode shapes used in the reduction procedure. Therefore, the reduced mass and stiffness matrices M_m and K_m will exactly predict all of the FEM dynamics in the frequency range spanned by the FEM modes used to reduce the model. A transformation of this type has been previously applied by Link[18] in the reduction of an incomplete system representation derived from test data to a system of order equal to the number of test mode shapes. Further details on the application of the method to nonsubstructured FEM representations can be found in Ref. 11.

Reduction of a Substructured FEM

In general, FEM representations of LSS will possess too many degrees of freedom to be processed as a single entity. The model is divided in a convenient way into several substructures. Each substructure is reduced to a set of dynamically important degrees of freedom, not necessarily physical, using any one of a number of available substructure representation techniques.[16,19-21] The reduced substructure representations are then assembled using methods of component mode synthesis.[22,23] System mode shapes are computed and modal coefficients for all physical degrees of freedom in each substructure can be recovered. The purpose of this section is to extend the modal reduction method to a substructured FEM resulting in a TAM containing only physical degrees of freedom that can be used in test-analysis correlation and system identification.

For a substructured FEM, the physical displacement vector u_n is partitioned into s subvectors

$$u_n = \{u_1^T:u_2^T:u_3^T:\cdots:u_s^T\}^T \tag{13}$$

where u_j corresponds to the displacement vector for the jth substructure. Likewise, the FEM modal matrix Φ_n is also partitioned according to substructure as

$$\Phi_n = \{\Phi_1^T:\Phi_2^T:\Phi_3^T:\cdots:\Phi_s^T\}^T \tag{14}$$

The system modal expansion given by Eq. (9) will then yield a corresponding expansion for each substructure of the form

$$u_j = \Phi_j\,q \qquad j = 1,s \tag{15}$$

Mass and stiffness matrices M_j and K_j are assembled for each substructure corresponding to the displacement vector u_j.

Substructures can be reduced to the physical degrees of freedom at the sensor location, which fall within each substructure. We proceed by partitioning the displacement and mode shape subvectors for the jth substructure into an a set and complementary o set

$$u_j = \{u_{ja}^T:u_{jo}^T\}^T \qquad \Phi_j = \{\Phi_{ja}^T:\Phi_{jo}^T\}^T \tag{16}$$

where the a set at the very least includes all degrees of freedom possessing sensors within the jth substructure and connection degrees of freedom to adjacent substructures. Using the procedure described for nonsubstructured models, a relation can be derived that expresses the o-set partition of the displacement in terms of the a-set partition

$$u_{jo} = \Phi_{jo}\,[\Phi_{ja}^T\Phi_{ja}]^{-1}\,\Phi_{ja}^T\,u_{ja} = D_j\,u_{ja} \tag{17}$$

This relationship is used to generate a transformation matrix $T_j = [I:D_j^T]^T$, which reduces the mass and stiffness matrices of the jth substructure to the reduced representation M_{jr} and K_{jr} containing only a-set degrees of freedom.

The reduced substructure representation M_{jr} and K_{jr} will exactly represent the response of the jth substructure within the system modes used in the reduction process. Reduced system mass and stiffness matrices are synthesized by assembling the reduced representations of all the substructures. The reduced system representation contains all of the a-set degrees of freedom from each of the upstream substructures. If degrees of freedom that do not possess sensors were included in the reduction of the substructures, they may be eliminated by further reducing the system to the TAM representation using the procedures that were applied to nonsubstructured models in the last section. The procedure described here for reducing a substructured FEM to a TAM representation has been successfully applied to several large models, including a static test configuration for the Space Shuttle solid rocket booster, described in Ref. 1.

For a nonsubstructured FEM, it was found that the modal reduction method could be implemented only if the matrix $A = [\Phi_a^T\Phi_a]$ was nonsingular. It turned out that this condition was not at all restrictive because the TAM degrees of freedom must be able to spatially distinguish between the system mode shapes if it is going to predict them at the reduced level. However, for a substructured FEM, the nonsingularity condition is shifted from the system level to the substructure level. Each of the matrices $A_j = [\Phi_{ja}^T\Phi_{ja}]$ must be nonsingular, which implies that the columns of Φ_{ja} must be linearly independent. Therefore, the sensor configuration within each substructure must be capable of spatially differentiating between each of the system modes. This condition has now become very restrictive and in many cases cannot be satisfied no matter how many sensors are placed within the offending substructure. For example, system modes that are of a local nature and contained entirely within a single substructure absolutely cannot be identified by sensors within the other substructures. In many cases, these localized modes are of great importance, such as in the instance of engine bending modes in a launch vehicle. In an attempt to relax the restriction imposed by the nonsingularity condition, we proceed by studying the equation of motion of the jth substructure

$$\begin{bmatrix} M_{jaa} & M_{jao} \\ M_{joa} & M_{joo} \end{bmatrix} \begin{Bmatrix} \ddot{u}_{ja} \\ \ddot{u}_{jo} \end{Bmatrix} + \begin{bmatrix} K_{jaa} & K_{jao} \\ K_{joa} & K_{joo} \end{bmatrix} \begin{Bmatrix} u_{ja} \\ u_{jo} \end{Bmatrix} = \begin{Bmatrix} F_{ja} \\ 0 \end{Bmatrix} \tag{18}$$

where we have partitioned the matrices into the a set, which now includes all the boundary degrees of freedom which interface with adjacent substructures, and the o set including all the degrees of freedom interior to the jth substructure. Note the only loads applied to the substructure are the interface loads at the boundary degrees of freedom.

A Craig-Bampton[16] representation of the substructure is generated for use in the synthesis of the system modes. The transformation to the Craig-Bampton representation is produced by considering two sets of independent substructure shapes as Ritz vectors. The first set of shapes are the constraint modes mentioned in the previous section. These static shapes are generated by considering the second equation of only the static portion of Eq. (18). Interior dynamics of the substructure are represented by mode shapes that are computed with the a-set degrees of freedom of the substructure

fixed. Details of the Craig-Bampton formulation can be found in Ref. 16.

The constraint modes and the fixed interface modes are combined to produce a relationship between the complete displacement vector of the substructure and the displacement vector of the Craig-Bampton representation

$$u_j = \left[\begin{array}{c:c} I & 0 \\ \hline -K_{joo}^{-1} K_{joa} & \Psi_o \end{array}\right] \left\{\begin{array}{c} u_{ja} \\ \hline q \end{array}\right\} = T_{jCB}\, u_{jCB} \tag{19}$$

where Ψ_o represents the fixed interface modes and q is the corresponding set of generalized coordinates. Reduced mass and stiffness matrices corresponding to the Craig-Bampton representation, M_{jCB} and K_{jCB}, respectively, are generated using a relation analogous to Eq. (6). The a-set partition of the Craig-Bampton displacement vector will not, in general, include the degrees of freedom within the substructure that are destined for the TAM. In addition, the Craig-Bampton representation of the substructure contains fixed interface modal coordinates q. These degrees of freedom cannot be monitored during the test and, therefore, must be removed. The Craig-Bampton representation of the substructure in its original form, although very accurate, is not adequate for use as a TAM.

The objective of the sequel is to adjust the Craig-Bampton substructure such that the new reduced displacement vector contains the original a-set degrees of freedom, for connection purposes, and the desired TAM degrees of freedom from the original o set. We proceed by splitting the o-set partitions of the jth substructure displacement vector u_j and the fixed interface mode shapes Ψ_o into two complementary sets t and x:

$$u_{jo} = \left\{\begin{array}{c} u_{jt} \\ \hline u_{jx} \end{array}\right\} \qquad \Psi_{jo} = \left\{\begin{array}{c} \Psi_{jt} \\ \hline \Psi_{jx} \end{array}\right\} \tag{20}$$

The t set contains all of the original o-set physical degrees of freedom, which are now to be placed in the TAM representation. The x set contains the remaining o-set degrees of freedom, which will still be omitted. The objective is to eliminate the generalized degrees of freedom q from the Craig-Bampton representation while retaining the t set in the new reduced representation. Examining the modal expansion for the t set in the fixed interface modes $u_{jt} = \Psi_t\, q$, we can use the generalized inverse to solve for the modal coordinates q yielding

$$q = [\Psi_{jt}^T\, \Psi_{jt}]^{-1} \Psi_{jt}^T\, u_{jt} \tag{21}$$

We can now generate a transformation R_j relating the Craig-Bampton displacement vector u_{jCB} to the displacement vector for the TAM representation of the jth substructure u_{jTAM} given by

$$u_{jCB} = \left\{\begin{array}{c} u_{ja} \\ \hline q \end{array}\right\} = \left[\begin{array}{c:c} I & 0 \\ \hline 0 & [\Psi_{jt}^T\, \Psi_{jt}]^{-1} \Psi_{jt}^T \end{array}\right] \left\{\begin{array}{c} u_{ja} \\ \hline u_{jt} \end{array}\right\} = R_j\, u_{jTAM} \tag{22}$$

The mass and stiffness matrices for the TAM representation of the jth substructure are then computed using the expressions

$$M_{jTAM} = R_j^T\, M_{jCB}\, R_j \qquad K_{jTAM} = R_j^T\, K_{jCB}\, R_j \tag{23}$$

A system representation is synthesized from all of the substructure TAM representations. The system can then be further reduced to the system TAM using the original modal reduction method for a nonsubstructured model. A distinct advantage of the modal reduction method just proposed is that it minimizes the amount of additional computation that must be performed beyond the modal analysis of the FEM to produce the system TAM representation. It utilizes the Craig-Bampton substructure representations, which were already

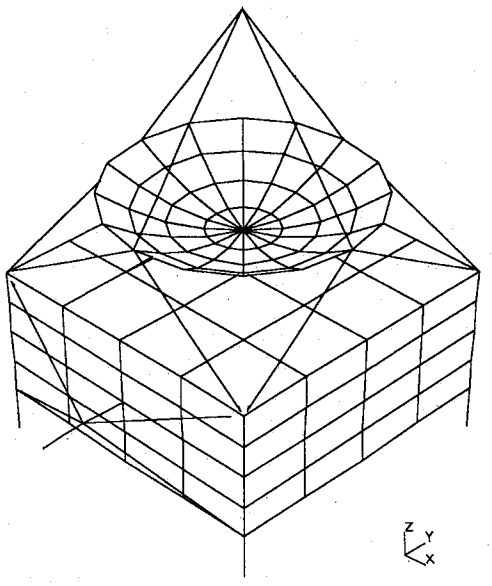

Fig. 1 Sample problem included 196 grid points (1176 degrees of freedom) and 267 elements.

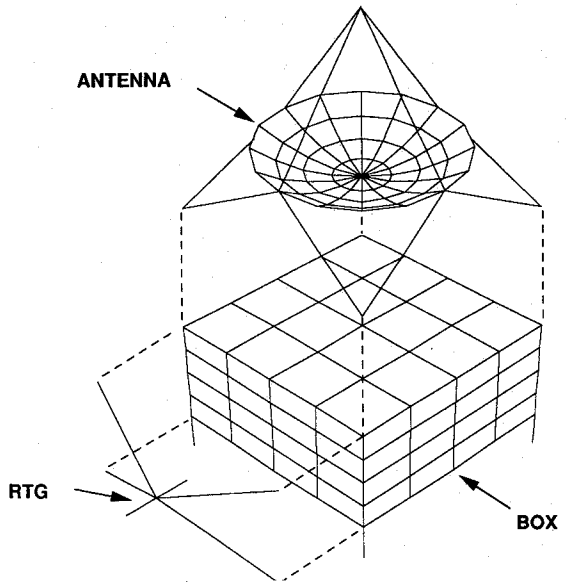

Fig. 2 Sample problem was divided into three substructures.

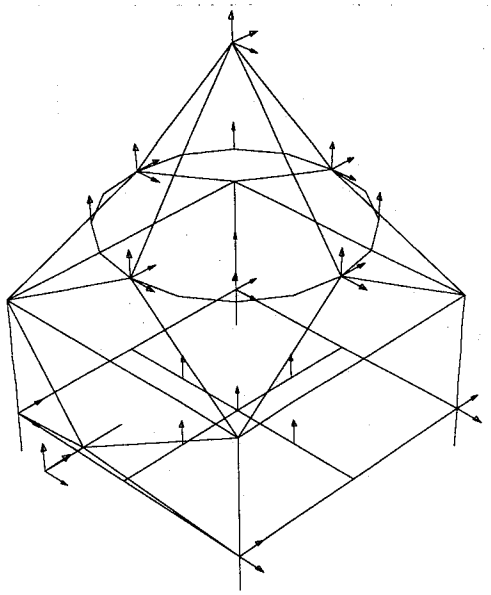

Fig. 3 Sample problem was reduced to 37 degrees of freedom.

Table 1 Component modal frequencies, Hz

Mode	Antenna	Box	RTG
1	24.501	14.997	18.026
2	24.502	30.433	21.671
3	29.215	36.608	——
4	45.890	37.005	——
5	45.890	——	——

Table 2 System mode frequencies, Hz, and strain energy fractions

Mode no.	Frequency, Hz	Antenna	Box	RTG
1	14.928	0.000	0.996	0.004
2	17.902	0.000	0.013	0.987
3	20.843	0.001	0.042	0.956
4	23.875	0.974	0.024	0.002
5	24.242	0.972	0.028	0.000
6	29.178	0.997	0.003	0.000
7	30.268	0.000	0.986	0.014
8	36.517	0.000	1.000	0.000
9	36.710	0.000	0.978	0.022
10	40.595	0.136	0.580	0.284
11	43.066	0.644	0.352	0.004
12	44.818	0.736	0.103	0.161
13	49.154	0.332	0.661	0.007
14	53.044	0.108	0.605	0.287

Table 3 System frequency errors for the static TAM

Mode no.	FEM	Static TAM	Error, %
1	14.928	14.975	0.31
2	17.902	17.902	0.00
3	20.843	20.843	0.00
4	23.875	24.329	1.90
5	24.242	24.314	0.30
6	29.178	29.280	0.35
7	30.268	31.483	4.01
8	36.517	38.443	5.27
9	36.71	38.560	5.04
10	40.595	40.535	-0.15
11	43.066	43.276	0.49
12	44.818	44.904	0.19
13	49.154	49.363	0.43
14	53.044	52.889	-0.29

computed for the FEM modal analysis, by performing a simple transformation to yield the TAM.

It is important to note that the proposed method of reduction still requires the inversion of the matrix $A_{jt} = [\Psi_{jt}^T \Psi_{jt}]$. This means that the sensor locations within a substructure must be capable of spatially differentiating between the fixed interface modes for the substructure. The immediate question is if this new condition is more or less restrictive than the nonsingularity condition that was imposed by the original substructured FEM reduction method. This condition is certainly much less restrictive because we have shifted the requirement from being capable of locally identifying a global mode shape to locally identifying a local mode shape. The sensor configuration within a substructure only has to be able to identify the dynamics within that substructure. Therefore this revised method meets our objective.

Regardless of the formulation, the modal-reduction method of TAM generation offers a valuable alternative to the commonly used Guyan reduction method in cases where structural mass and frequency characteristics result in an inaccurate static reduction. Because the method results in an exact reduction, TAM uncertainty is eliminated from test-analysis correlation and system identification. Errors found in the test-analysis correlation can, then, be directly attributed to either inaccuracies in the FEM or errors in the test data. The frequency range over which the TAM is dynamically valid can be easily controlled by adding or removing FEM modes from the reduction process. This capability may prove to be very important for LSS, where there may be literally hundreds of mode shapes in the frequency range of interest but only a relative few which are dynamically important. Another advantage of the proposed method is the fact that only a relatively small matrix $A_{jt} = [\Psi_{jt}^T \Psi_{jt}]$ must be inverted, therefore, the modal reduction method is not computationally intensive.

Numerical Application

To demonstrate the application of the new modal reduction method formulation for substructured models, a simple problem was analyzed. The model considered represented a communication satellite or interplanetary spacecraft weighing approximately 5726 pounds. Three main components, an instrumentation bus (box), a communication antenna, and a power generator make up the example spacecraft. Each of these components was represented by an individual substructure. The FEM representation is illustrated in Fig. 1. Individual substructures are shown in Fig. 2. The complete model contained 196 grid points, 1176 degrees of freedom, and 267 elements.

Component modes were calculated for each substructure to a frequency of 55 Hz. The box component had four modes between 15.0 and 37.0 Hz. The antenna had five modes between 24.5 and 45.9 Hz. Finally, the power generator had only two component modes at 18.0 and 21.7 Hz. The component modal frequencies for all three substructures are summarized in Table 1. System modes of the spacecraft were calculated by assembling the three substructures using the Craig-Bampton modal synthesis technique.[16] The base of the spacecraft legs (the interface to the launch vehicle) were restrained in all six degrees of freedom. Fourteen system modes were calculated, with frequencies between 14.9 and 53.0 Hz. System modal frequencies, along with substructure strain energy fractions, are listed in Table 2.

The next step following the calculation of the component and system modes was to create the TAM representation. A sufficient number of accelerometer locations were selected such that all system modes could be spatially differentiated. A total of 34 sensor locations were selected, including 14 on the box, 20 on the antenna, and three on the power generator. Selected accelerometer locations are illustrated in Fig. 3.

An initial TAM was created using the traditional method of static (Guyan) reduction. This method is insensitive to whether or not substructuring is used because the same transformation is employed for both the component and system reductions. Since this method does not include any mass effects in the transformation matrix, it might be expected that the static TAM would develop some errors during the reduction. This was indeed the case. FEM/TAM frequency agreement was reasonably good, as listed in Table 3. However, several mode shapes of the static TAM were significantly different than the complete FEM representation. This can be seen in the cross-orthogonality computation results, presented in Table 4.

The next attempt to create a TAM was made using the original system modal TAM formulation[11] extended to the substructure level. This approach immediately encountered difficulties. For the power generator, there were only three accelerometers; this was clearly an insufficient number to spatially differentiate between all fourteen system mode shapes. Thus, matrix $A_j = [\Phi_{ja}^T \Phi_{ja}]$ found in the modal TAM transformation of Eq. (17) is singular and cannot be inverted. Similar problems existed for the antenna. Two of the system modes were dominated by plate bending of the upper and lower panels of the instrumentation box. From the sensor locations on the antenna, these two modes had essentially identical shapes. Therefore, matrix A_j was poorly conditioned and not accurately invertible.

The final TAM was created using the new modal reduction formulation for substructured models presented in this paper. In this approach, the accelerometers on each component must be capable of spatially differentiating between the component

Table 4 Cross-orthogonality for static TAM

FEM mode no.	FEM frequency	Maximum x-ortho	TAM mode	Next largest x-ortho	TAM mode
1	14.928	0.994	1	0.00005	2
2	17.902	1.000	2	0.00007	1
3	20.843	1.000	3	0.00052	5
4	23.875	0.994	4	0.00214	11
5	24.242	0.994	5	0.00062	10
6	29.178	0.993	6	0.00053	7
7	30.268	0.922	7	0.00964	10
8	36.517	0.894	8	0.00888	11
9	36.710	0.888	9	0.116	10
10	40.595	0.977	10	0.152	9
11	43.066	0.987	11	0.0152	8
12	44.818	0.984	12	0.0417	9
13	49.154	0.985	13	0.0110	8
14	53.044	0.988	14	0.0279	12

Table 5 System frequencies for the substructured modal TAM

Mode no.	FEM	Static TAM	Error, %
1	14.928	14.928	0.00
2	17.902	17.902	0.00
3	20.843	20.843	0.00
4	23.875	23.875	0.00
5	24.242	24.242	0.00
6	29.178	29.178	0.00
7	30.268	30.268	0.00
8	35.517	36.517	0.00
9	36.710	36.710	0.00
10	40.595	40.595	0.00
11	43.066	43.066	0.00
12	44.818	44.818	0.00
13	49.154	49.154	0.00
14	53.044	53.044	0.00

Table 6 Cross-orthogonality for the substructured modal TAM

FEM mode no.	FEM frequency	Maximum x-ortho	TAM mode	Next largest x-ortho	TAM mode
1	14.928	1.000	1	—	—
2	17.902	1.000	2	—	—
3	20.843	1.000	3	—	—
4	23.875	1.000	4	—	—
5	24.242	1.000	5	—	—
6	29.178	1.000	6	—	—
7	30.268	1.000	7	—	—
8	36.517	1.000	8	—	—
9	36.710	1.000	9	—	—
10	40.595	1.000	10	—	—
11	43.066	1.000	11	—	—
12	44.818	1.000	12	—	—
13	49.154	1.000	13	—	—
14	53.044	1.000	14	—	—

mode shapes rather than the system mode shapes. Because of this more reasonable requirement, the substructured modal TAM formulation worked extremely well for all spacecraft components. The resulting modal TAM showed excellent agreement with the original FEM representation. FEM/TAM frequency agreement was exact within numerical accuracy, as listed in Table 5. Mode shape correlation was also exact, as indicated by the FEM/TAM cross-orthogonality results presented in Table 6. This example demonstrates that the new modal reduction formulation for substructured models preserves the accuracy of the original modal TAM approach and includes convenient extensions for easily processing large substructured models.

Conclusion

The modal TAM procedure has been revised to work with substructured finite element models. Sensor locations within each component must be selected such that they are capable of spatially differentiating between the component mode shapes rather than the system mode shapes. This is an important extension for FEM representations of large space structures that are often formed of extremely detailed substructures with weak coupling between different components.

The new method was applied to a simple but representative example of a communications satellite or interplanetary spacecraft with a FEM containing three substructures. Due to the relatively large number of accelerometers used, the static reduction method provided a reasonably accurate TAM representation in this case. A straightforward application of the original modal reduction method resulted in the inability to spatially differentiate between the system mode shapes at the power generator and antenna substructure levels.

The new modal reduction formulation for substructured models resulted in a TAM representation that exactly predicted the FEM frequencies and mode shapes to within numerical accuracy. The new formulation retains the exact FEM representation of the original modal TAM method compared to the approximate representation of the traditional static reduction.

References

[1]Brillhart, D., Kammer, D. C., Hunt, D. L., and Hurst, G., "Dynamic Verification of the Space Shuttle T-97 SRM Static Firing Test Stand," *Proceedings of the 7th International Modal Analysis Conf.*, Las Vegas, NV, Jan. 1989.

[2]Kammer, D. C., Jensen, B. M., and Mason, D. R., "Test-analysis Correlation of the Space Shuttle Solid Rocket Motor Center Segment," *Journal of Spacecraft and Rockets*, Vol. 26, No. 4, July 1989, pp. 266–273.

[3]Chen, J. C., and Garba, J. A., "Structural Analysis Model Validation Using Modal Test Data," *Combined Experimental/Analytical Modeling of Dynamic Structural Systems,* Applied Mechanics Division, Vol. 67, ASME, 1985, pp. 109–137.

[4]Kabe, A., "Stiffness Matrix Adjustment Using Mode Data," *AIAA Journal,* Vol. 23, Sept. 1985, pp. 1431–1436.

[5]Berman, A., Wei, F., and Rao, K. V., "Improvement of Analytical Dynamic Models Using Modal Test Data," *Proceedings of the 21st AIAA Structures, Structural Dynamics, and Materials Conf.*, Paper No. 80-0800, 1980, pp. 809–814.

[6]Kammer, D. C., "An Optimum Approximation for Residual Stiffness in Linear System Identification," *AIAA Journal,* Vol. 26, Jan. 1988, pp. 104–112.

[7]Flanigan, C. C., "Test/Analysis Correlation of the STS Centaur Using Design Sensitivity and Optimization Methods," *Proceedings of the 5th International Modal Analysis Conf.*, London, England, April 1987, pp. 99–107.

[8]Kammer, D. C., Flanigan, C. C., and Dreyer, W., "A Superelement Approach to Test Analysis Model Development," *Proceedings of the 4th International Modal Analysis Conf.*, Los Angeles, CA, Feb. 1986, pp. 663–673.

[9]Ewins, D. J., *Modal Testing: Theory and Practice,* Wiley, New York, 1984.

[10]Coppolino, R. N., Bendat, J. S., and Stroud, R. C., "New Processor Integrates Dynamic Testing and Analysis," *Sound and Vibration,* Aug. 1986, pp. 16–22.

[11]Kammer, D. C., "Test-Analysis Model Development Using an Exact Modal Reduction," *The International Journal of Analytical and Experimental Modal Analysis,* Oct. 1987, pp. 174–179.

[12]Kuhar, E. J., and Stahle, C. V., "A Dynamic Transformation Method for Modal Synthesis," *Proceedings of the AIAA/ASME/SAE 14th Structures, Structural Dynamics, and Materials Conf.*, Mar. 1973.

[13]Paz, M., "Dynamic Condensation," *AIAA Journal,* Vol. 22, May 1984, pp. 724–727.

[14]Miller, C. A., "Dynamic Reduction of Structural Models," *Journal Struct. Div. ASCE,* 1980, pp. 2097–2108.

[15]Guyan, R. J., "Reduction of Mass and Stiffness Matrices," *AIAA Journal,* Vol. 3, No. 2, 1965, p. 380.

[16]Craig, R. R., Jr., and Bampton, M. C. C., "Coupling of Substructures for Dynamic Analysis," *AIAA Journal,* Vol. 6, No. 7, 1968, pp. 1313–1319.

[17]Penrose, R., "A Generalized Inverse for Matrices," *Proceedings for the Cambridge Philosophical Society,* Vol. 51, 1955, p. 406–413.

[18]Link, M., "Identification of Physical System Matrices Using

Incomplete Vibration Data," *Proceedings of the 4th International Modal Analysis Conf.*, Union College, Los Angeles, CA, Feb. 1986.

[19]Kammer, D. C., and Baker, M., "A Comparison of the Craig-Bampton and Residual Flexibility Methods for Component Substructure Representation," *Journal of Aircraft*, Vol. 24, April 1987, pp. 262-267.

[20]Rubin, S., "An Improved Component-Mode Representation," *Proceedings of the AIAA/ASME/SAE 15th Structures, Structural Dynamics, and Materials Conf.*, Las Vegas, NV, April 1974.

[21]Craig, R. R., and Chang, C. J., "On the Use of Attachment Modes in Substructure Coupling for Dynamic Analysis," *Proceedings of the AIAA/ASME 18th Structures, Structural Dynamics, and Materials Conf.*, 1977, pp. 89-99.

[22]Craig, R. R., "A Review of Time-Domain and Frequency-Domain Component Synthesis Methods," *Combined Experimental/Analytical Modeling of Dynamic Structural Systems*, Applied Mechanics Division, Vol. 67, ASME, 1985, pp. 1—30.

[23]Hintz, R. M., "Analytical Methods in Component Modal Synthesis," *AIAA Journal*, Vol. 13, Aug. 1975, pp. 1007-1016.

David H. Allen
Associate Editor